# Status and prospects of the DEAP-3600 experiment

**Vicente Pesudo**
(CIEMAT/LSC)
on behalf of the DEAP collaboration

LIDINE
Madrid, Spain, 20-22 September 2023

# Outline

Current picture and DEAP-3600 achievements

The DEAP-3600 experiment

Recovering sensitivity

Prospects

# Current picture and achievements of DEAP-3600

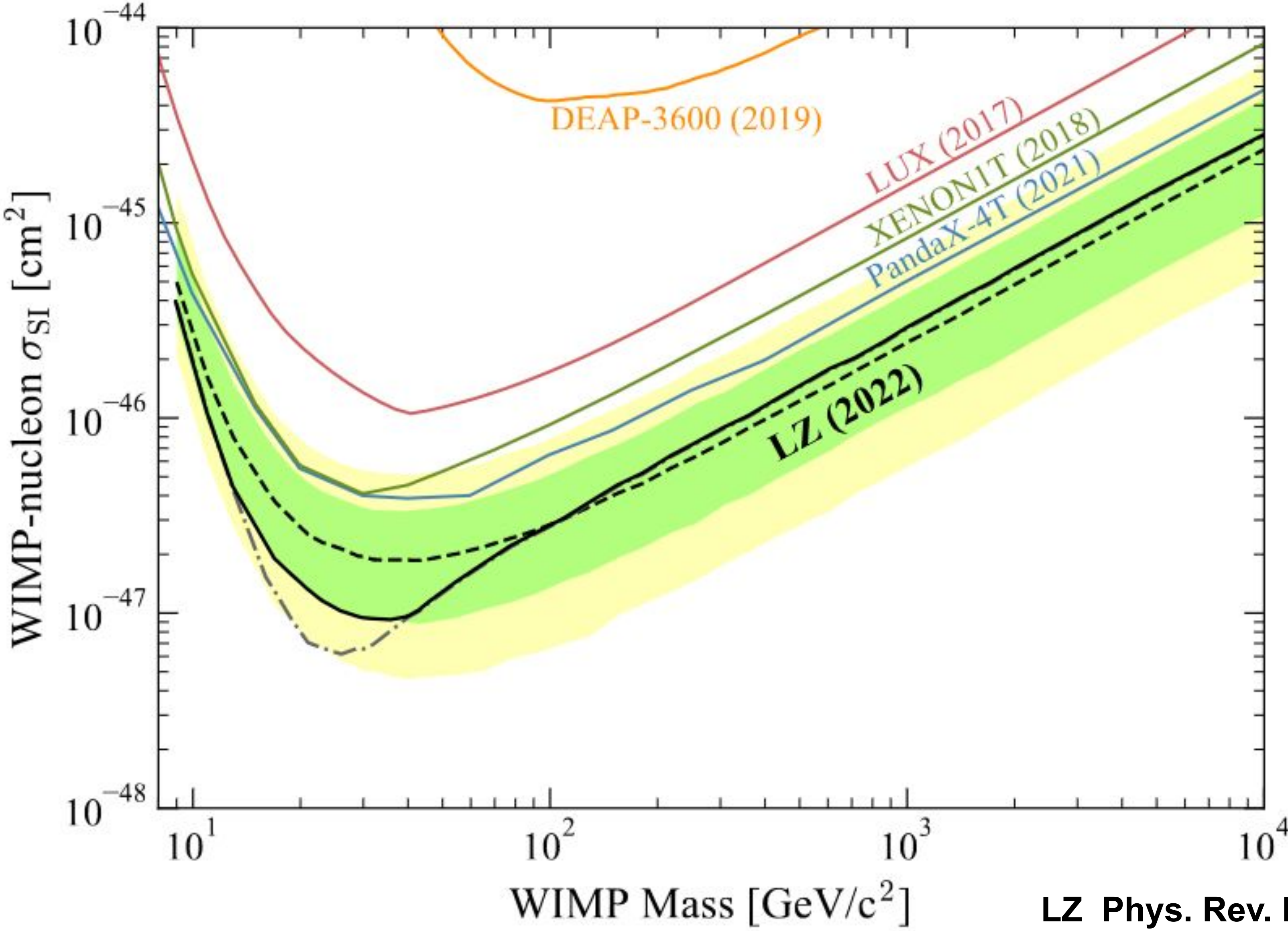


**LZ Phys. Rev. Lett. 131, 041002 (2023)**

# Current picture and achievements of DEAP-3600

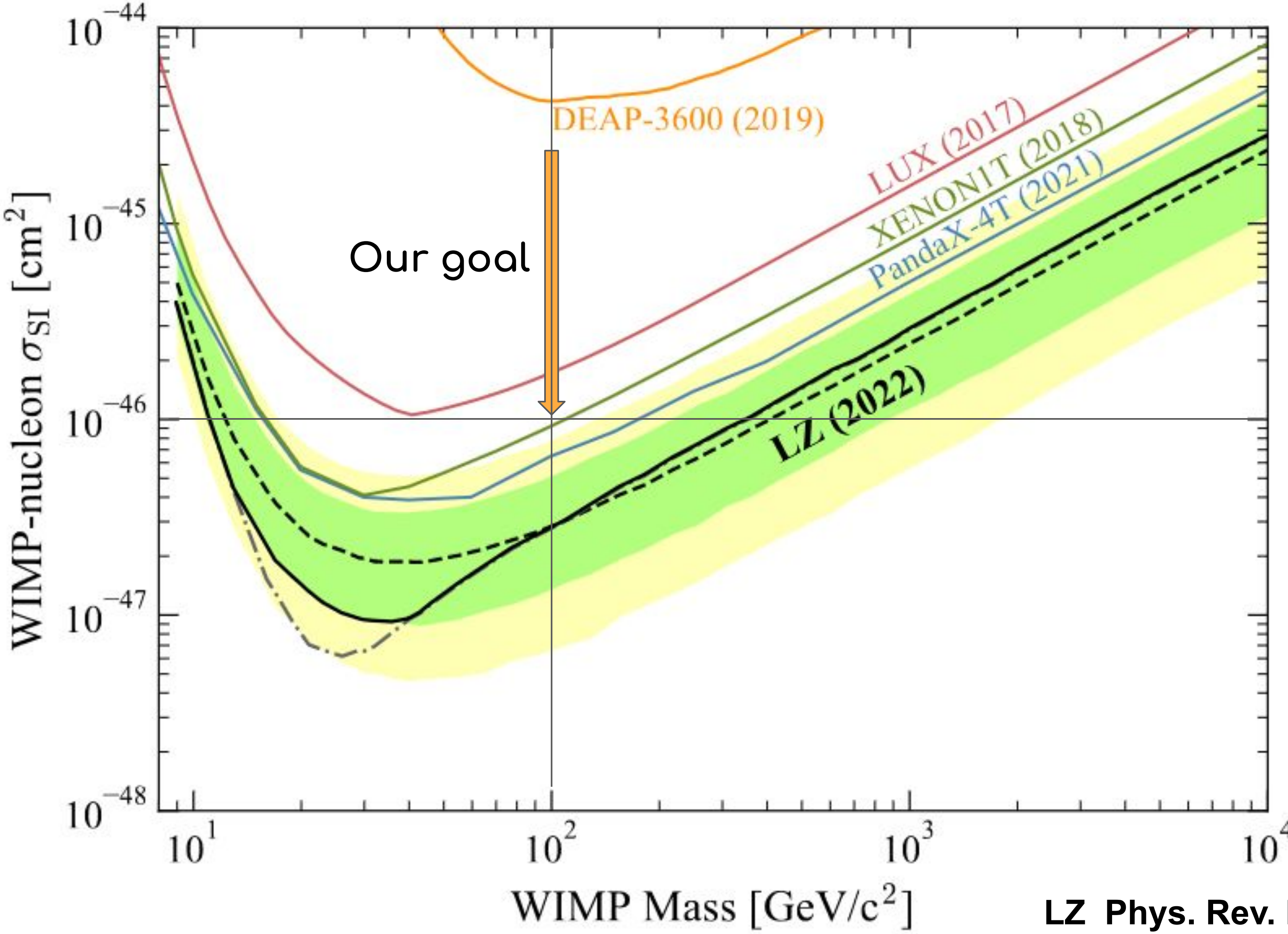


**LZ Phys. Rev. Lett. 131, 041002 (2023)**

# Current picture and achievements of DEAP-3600

First DM detector with a target > 1 tonne

Most stringent limits for standard WIMP SI interaction

with a:

- non-Xe target
- without a TPC
- in single phase

Potential path for next generation

# Current picture and achievements of DEAP-3600

More exotic DM scenarios already presented @ LIDINE last year by Michela Lai:

- Best limits for xenon-phobic DM Phys. Rev. D 102, 082001 (2020).
- Prospection of unpopulated regions of the parameter space at Planck-scale masses (ultra heavy) Phys. Rev. D, 100, 072009 (2019).

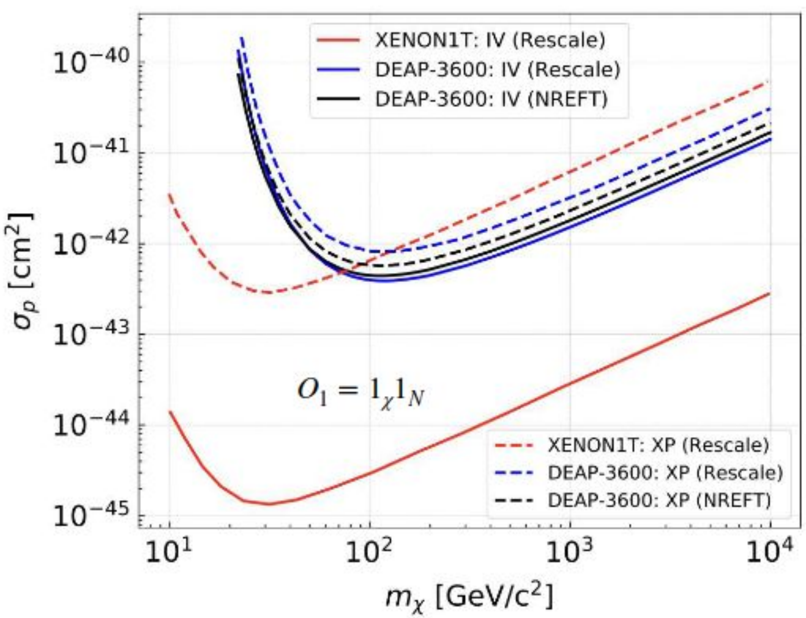


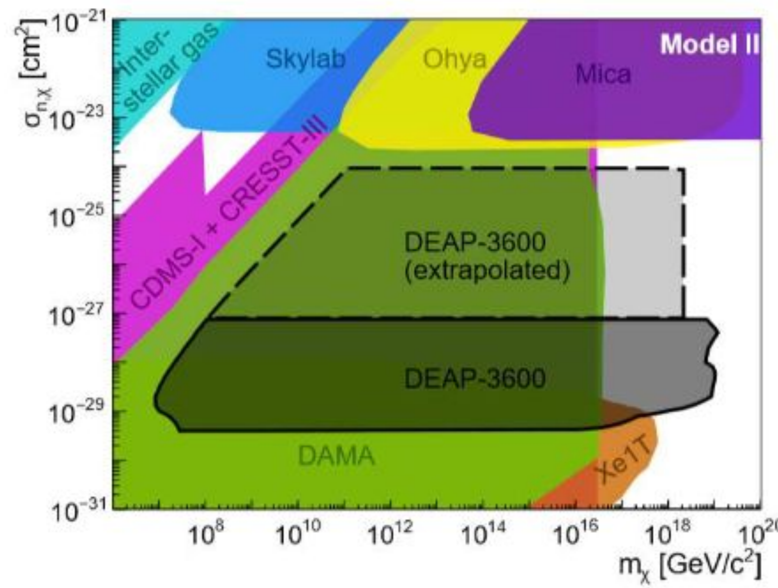

# The DEAP-3600 detector: Ar scintillation

- Singlet state   fast decay (~ns) dominantly populated by nuclear recoils
- Triplet state   slow decay (1.6 μs) dominantly populated by electronic recoils
- No electric field
- **Pulse shape allows us to discriminate** against gamma and beta backgrounds.
- Position reconstruction and fiducialization allow us to reduce surface and external backgrounds.

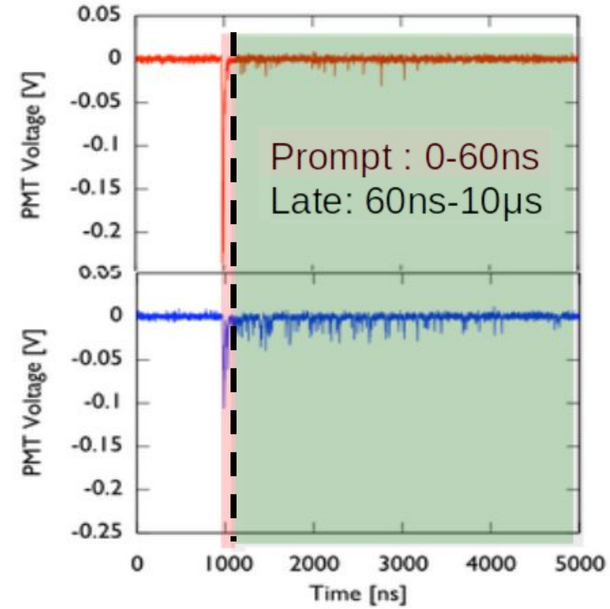


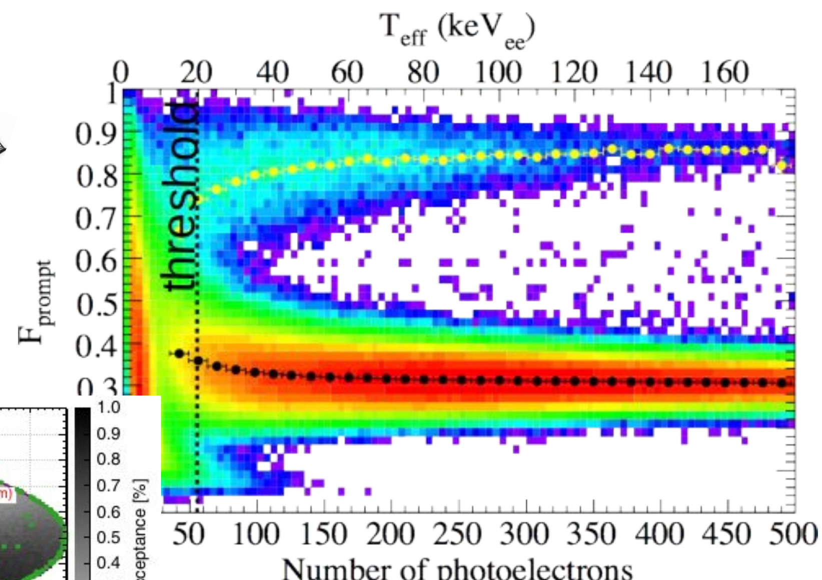


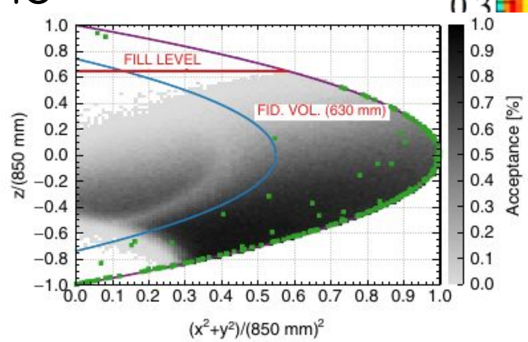

# The DEAP-3600 detector

- Singlet state   fast decay (~ns) dominantly populated by nuclear recoils
- Triplet state   slow decay (1.6 μs) dominantly populated by electronic recoils
- No electric field
- **Pulse shape allows us to discriminate** against gamma and beta backgrounds.
- Position reconstruction and fiducialization allow us to reduce surface and external backgrounds.

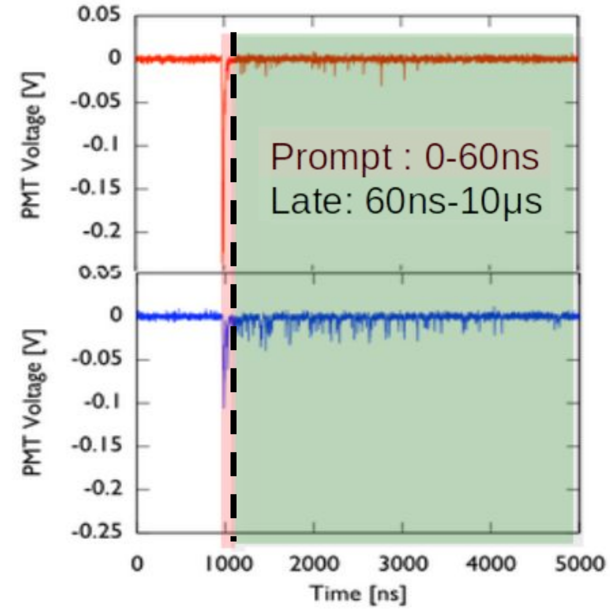


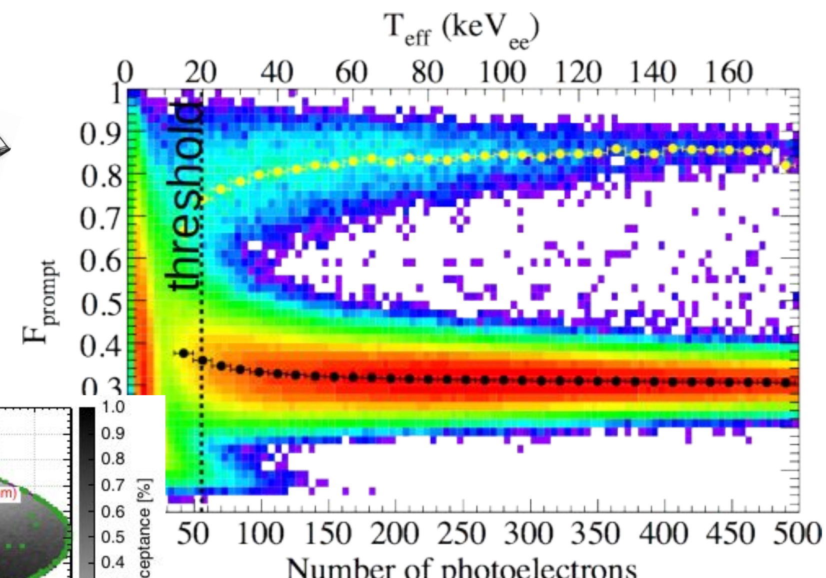


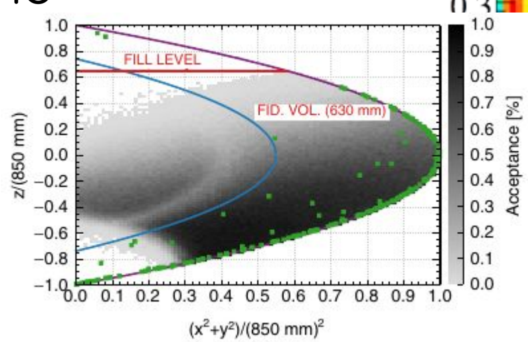


**Check Ludovico's poster!**

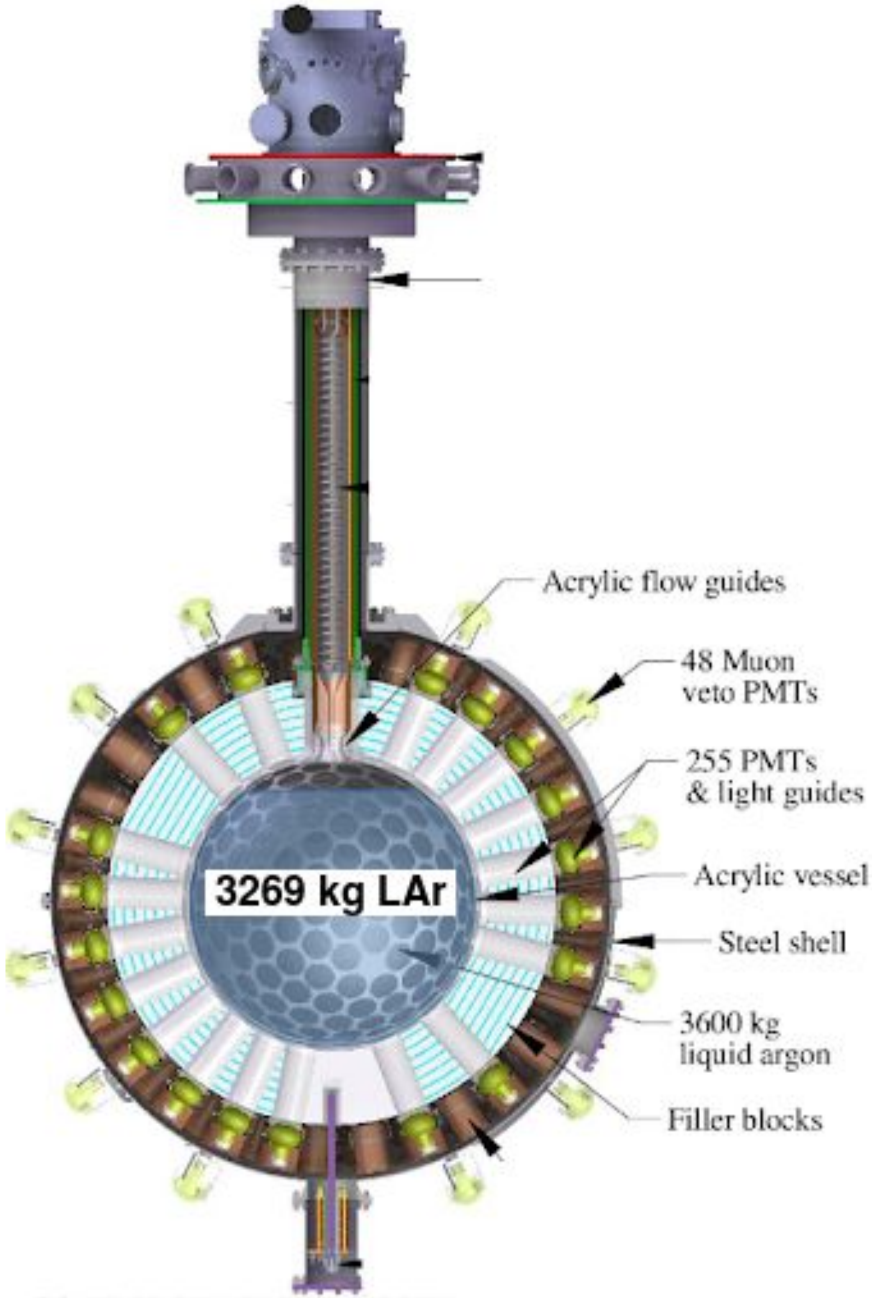


- 3.3 tonne LAr target in ultraclean acrylic vessel (R = 85 cm).
- In-situ vacuum evaporated TPB on inner 10 $m^2$ surface.
- Bonded 50-cm-long light guides: distance to PMTs
- 255 PMTs: Hamamatsu R5912 HQE. 8" - 32 % QE - 75% coverage.
- Immersed in water tank with PMTs to veto muons (Cherenkov light).
- Located 2 km underground @ SNOLAB: 6000 m.w.e -> 0.03 muon/m2/day

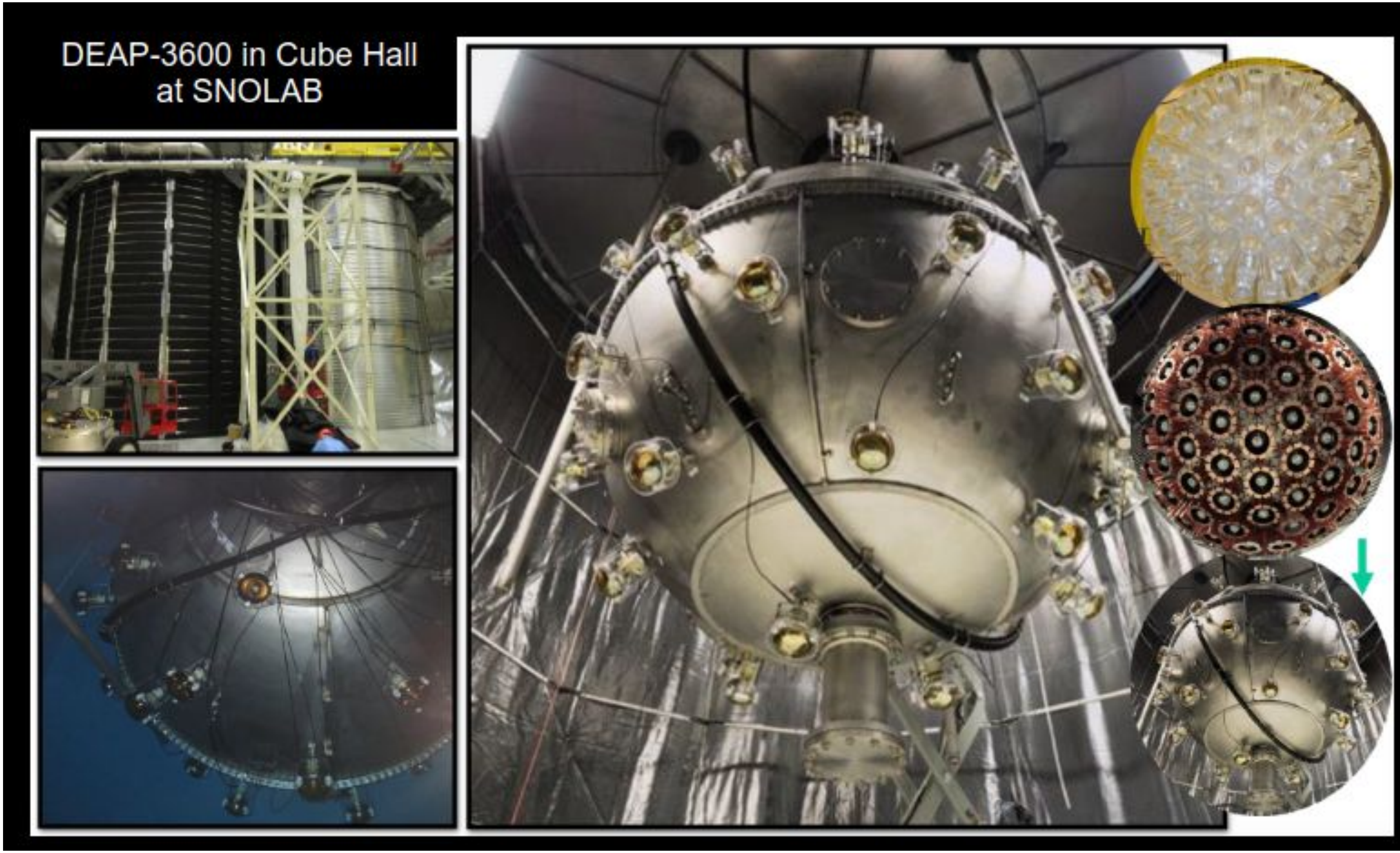
DEAP-3600 in Cube Hall
at SNOLAB

# Prospects in a nutshell

1. **Tackling limiting factors to WIMP sensitivity (hardware upgrades)**

2. **Finalize refined analyses** (better detector model + Profile likelihood + machine learning) **and unblind**

3. **Exploit this science machine and learn for DarkSide-20k, ARGO and beyond**

# Prospects in a nutshell

1. **Tackling limiting factors to WIMP sensitivity (hardware upgrades)**

2. **Finalize refined analyses** (better detector model + Profile likelihood + machine learning) **and unblind**

See Shawn's talk after the coffee break!

3. **Exploit this science machine and learn for DarkSide-20k, ARGO and beyond**

# Recovering sensitivity

Bkg 1: surface $^{210}Po$ on the neck (above target)

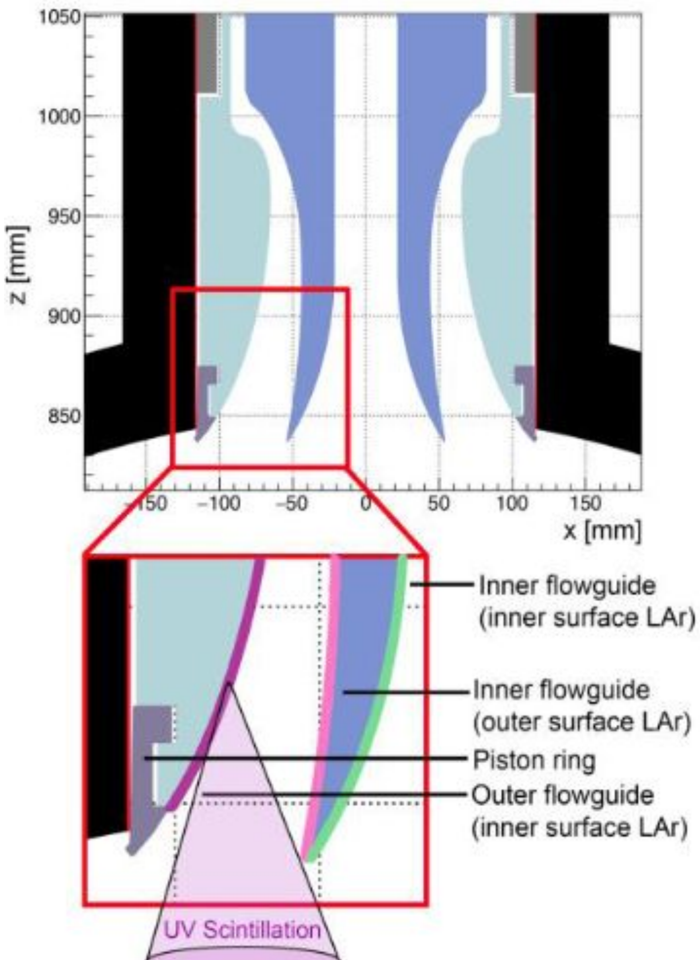


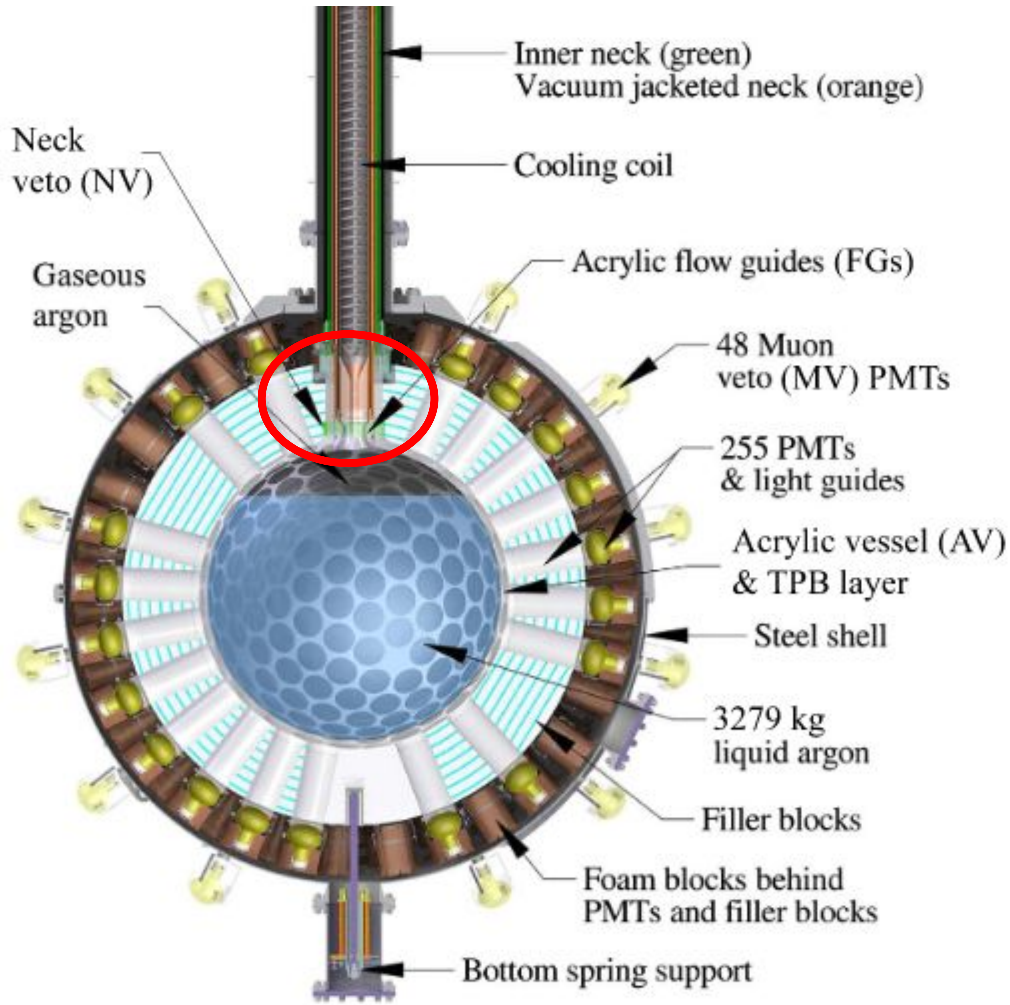


PRD, 100 (2019), p 022004

# Recovering sensitivity

Bkg 1: surface $^{210}Po$ on the neck (above target)

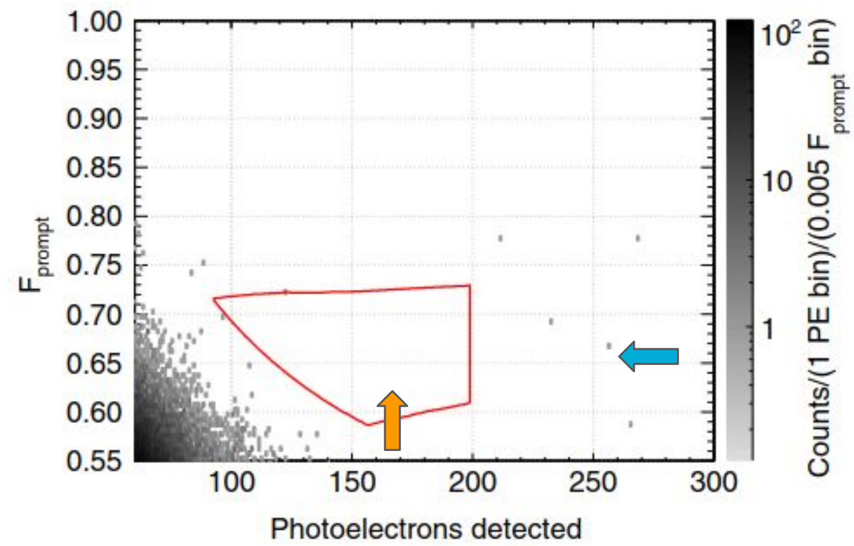


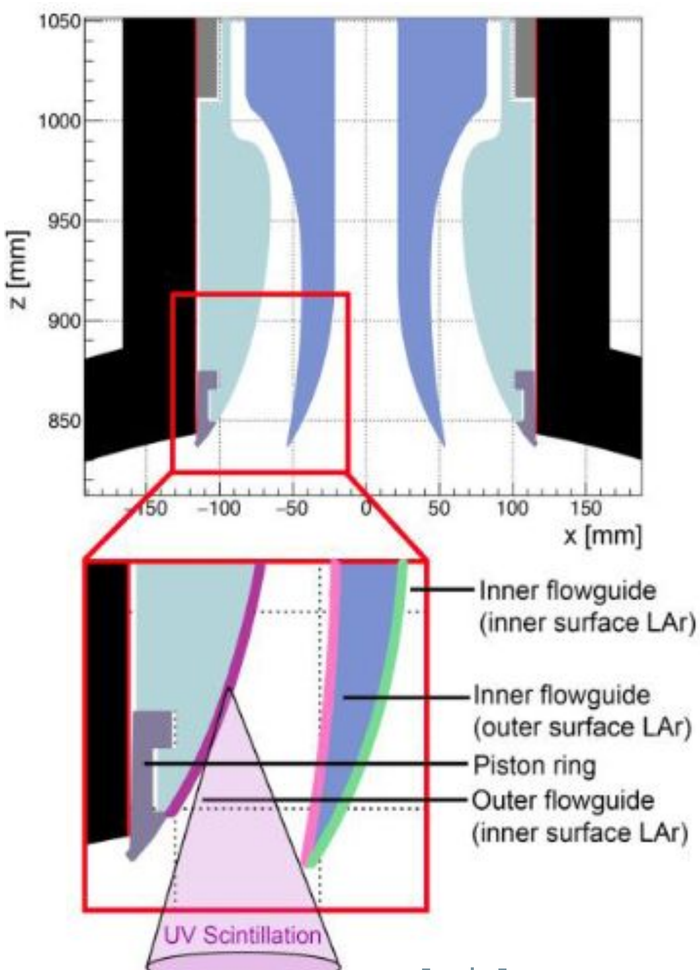


Unfortunate combination of:

- Surface activity
- Condensation on neck surf. ↑
- Many photons not detected ←
- Topologic pattern mimicking good NR events

PRD, 100 (2019), p 022004

# Recovering sensitivity

Bkg 1: surface $^{210}$Po on the neck (above target)

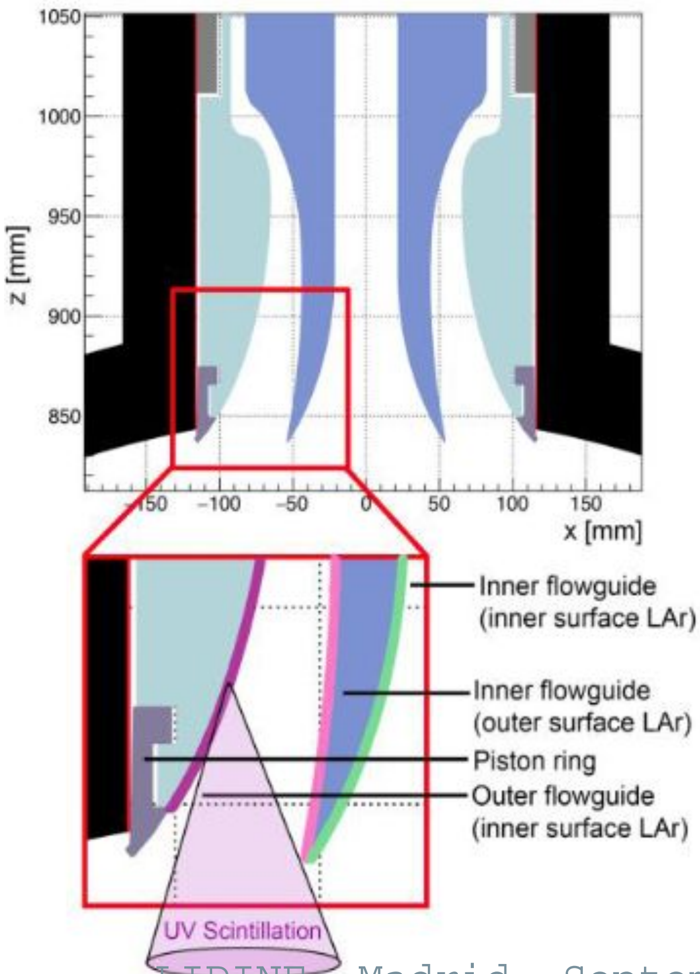


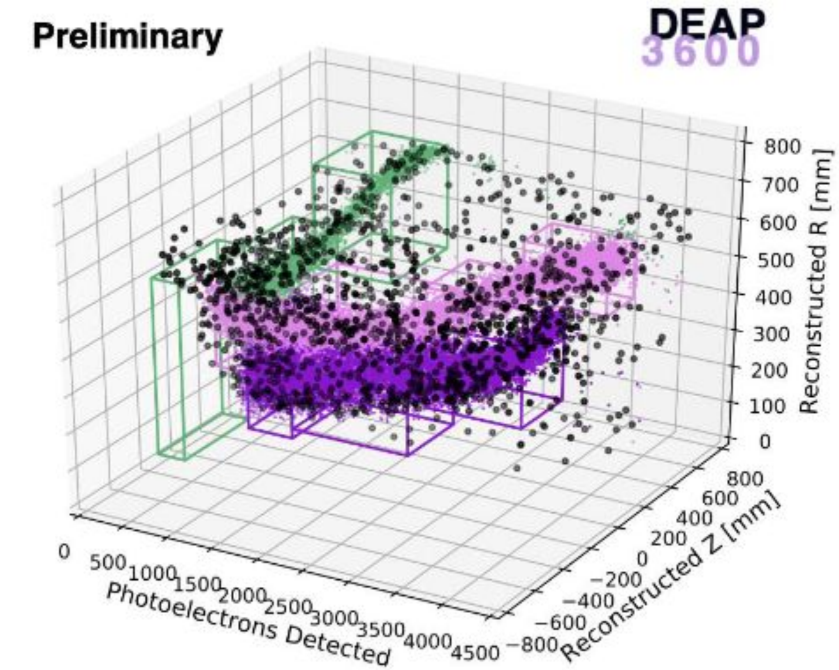


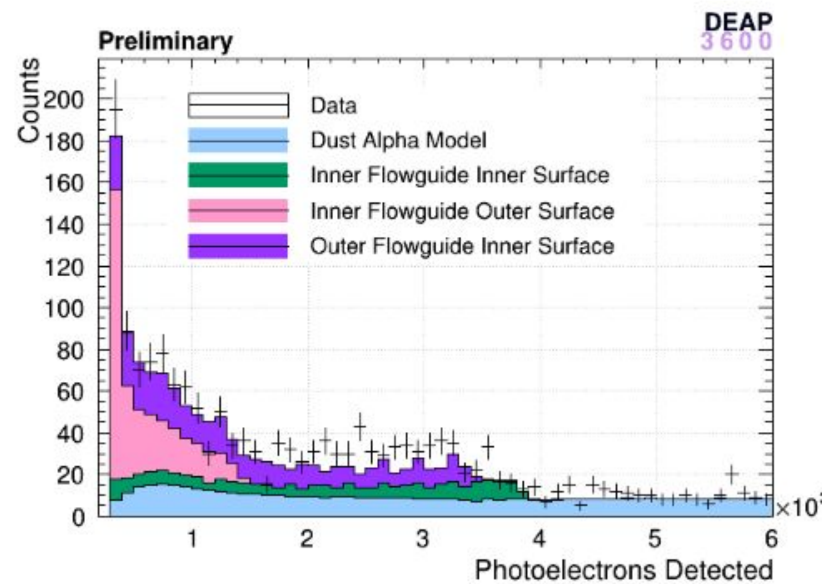

# Recovering sensitivity

Bkg 1: surface $^{210}Po$ on the neck (above target)

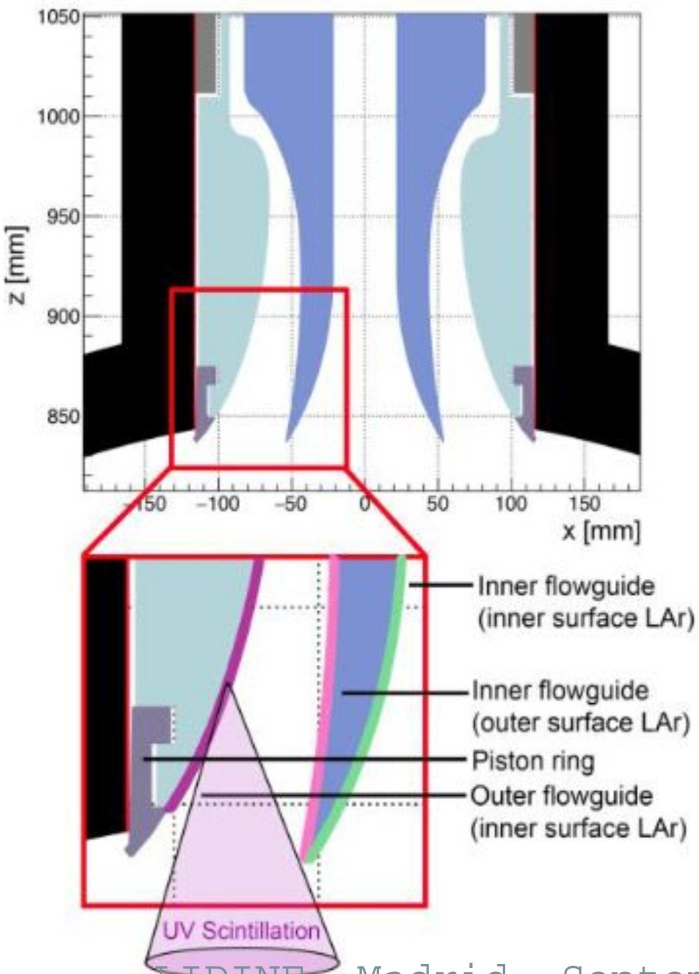


CNN trained against this bkg gives very good results!

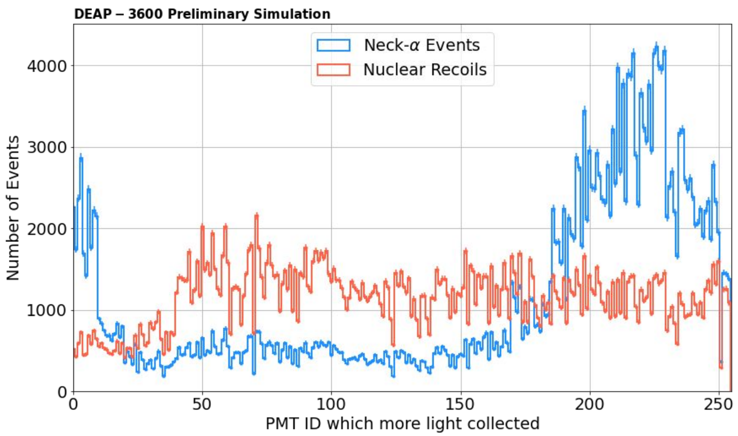


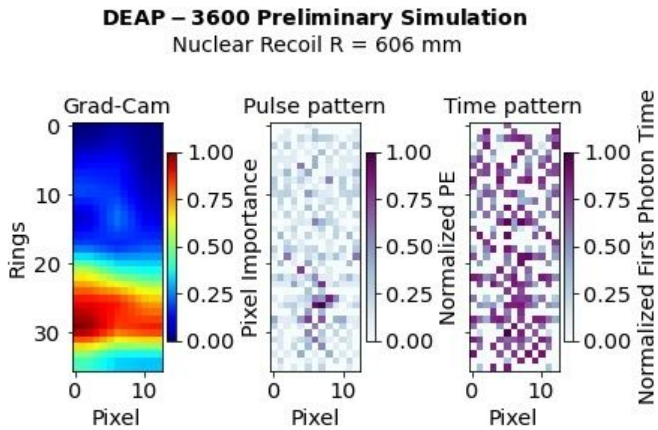


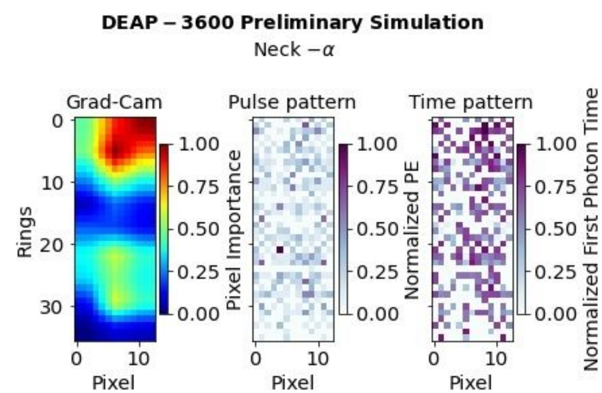

# Recovering sensitivity

Fix 1: WLS modifying the time profile of alpha scintillation

- Neck events will have a different time profile.
- distinct PSD pattern.
- More light collected.
- Out of the ROI.

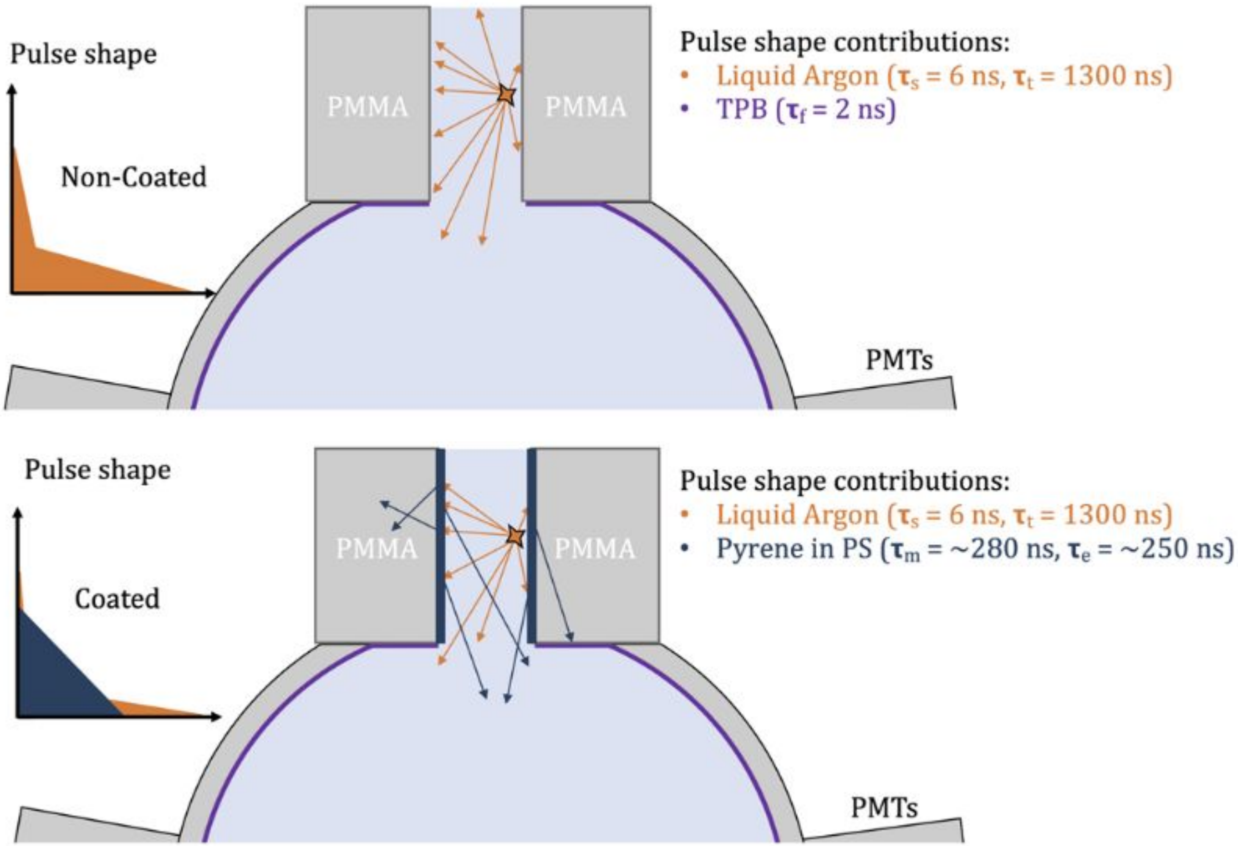


NIM A 1034 (2022) p 166683

# Recovering sensitivity

Fix 1: WLS modifying the time profile of alpha scintillation

- Neck events will have a different time profile.
- distinct PSD pattern.
- More light collected.
- Out of the ROI.

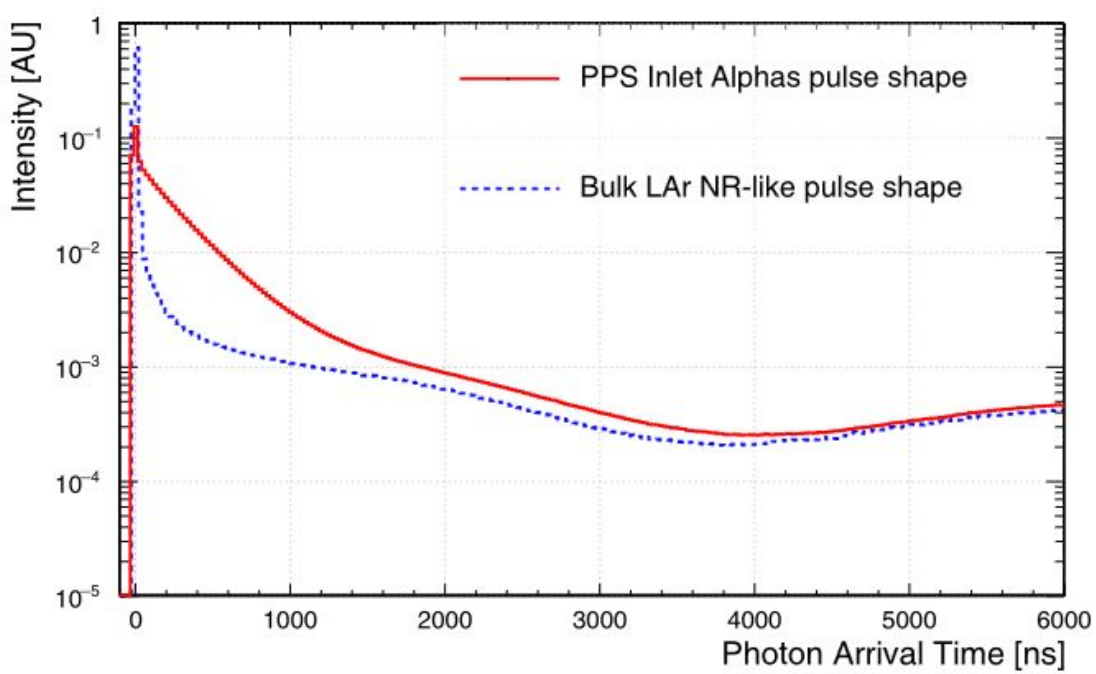


NIM A 1034 (2022) p 166683

# Hardware upgrades

- Deployment canister + hoist installed.
- Neck replacement in progress
- Neck seal fixed simultaneously

Allowing for full detector fill

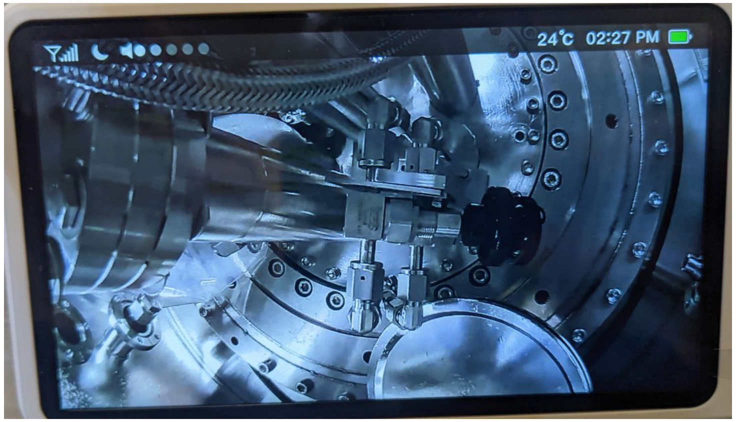


# Hardware upgrades

- Deployment canister + hoist installed.
- Neck replacement in progress
- Neck seal fixed simultaneously

Allowing for full detector fill


# Recovering sensitivity

Bkg 2: degraded alphas from dust particulates in suspension

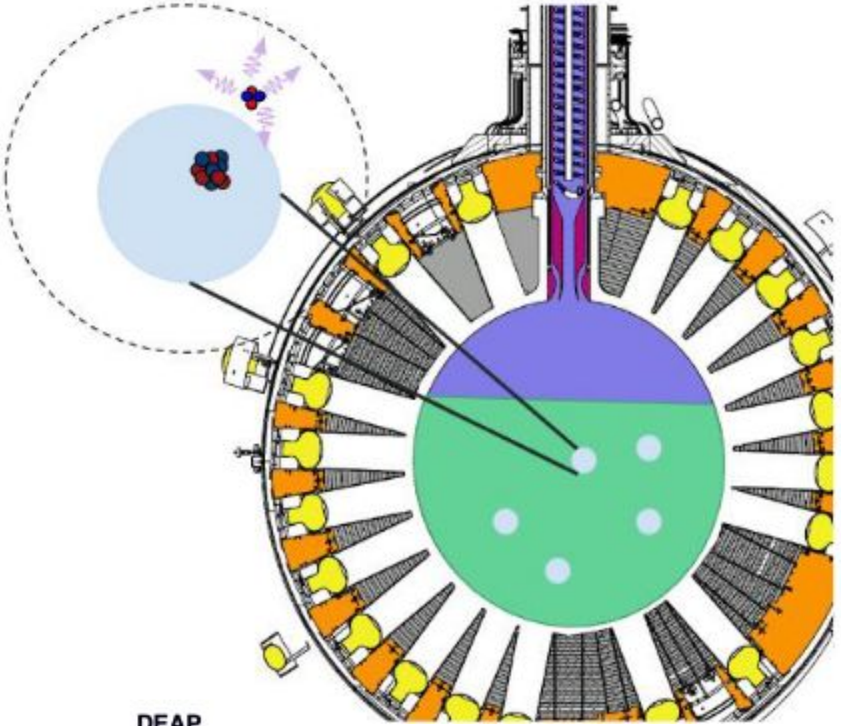

DEAP operated with no recirculation or filtration

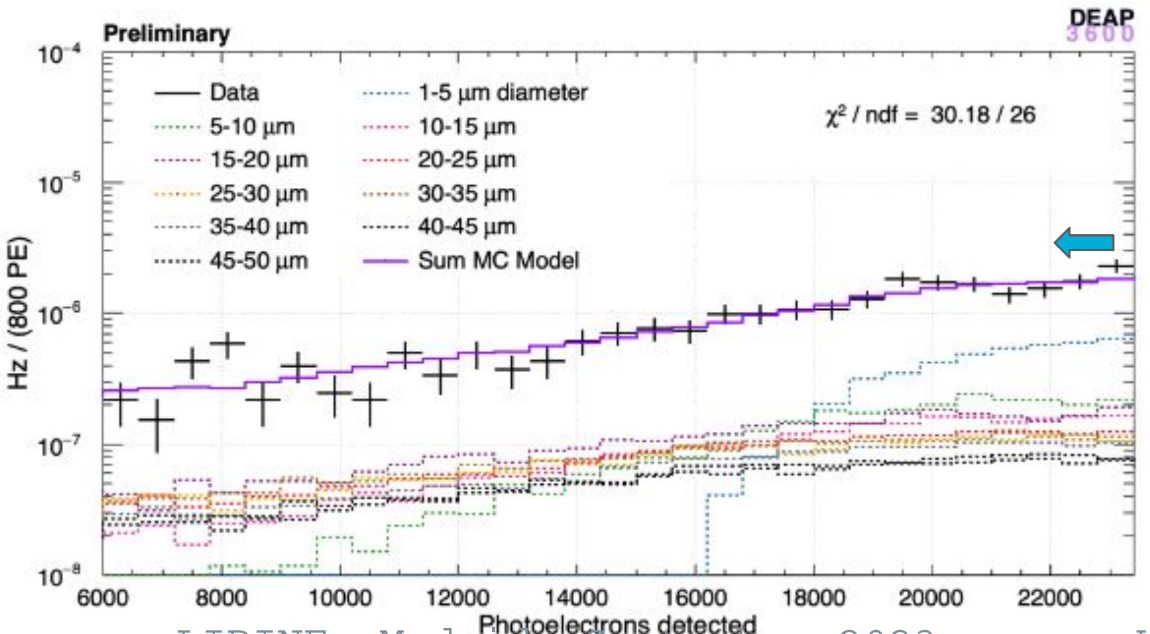


E lost in the dust itself does not produce photons.

# Recovering sensitivity

Fix 2: New recirculation+filtration system to remove dust from target

External cooling also prevents condensation in the neck!

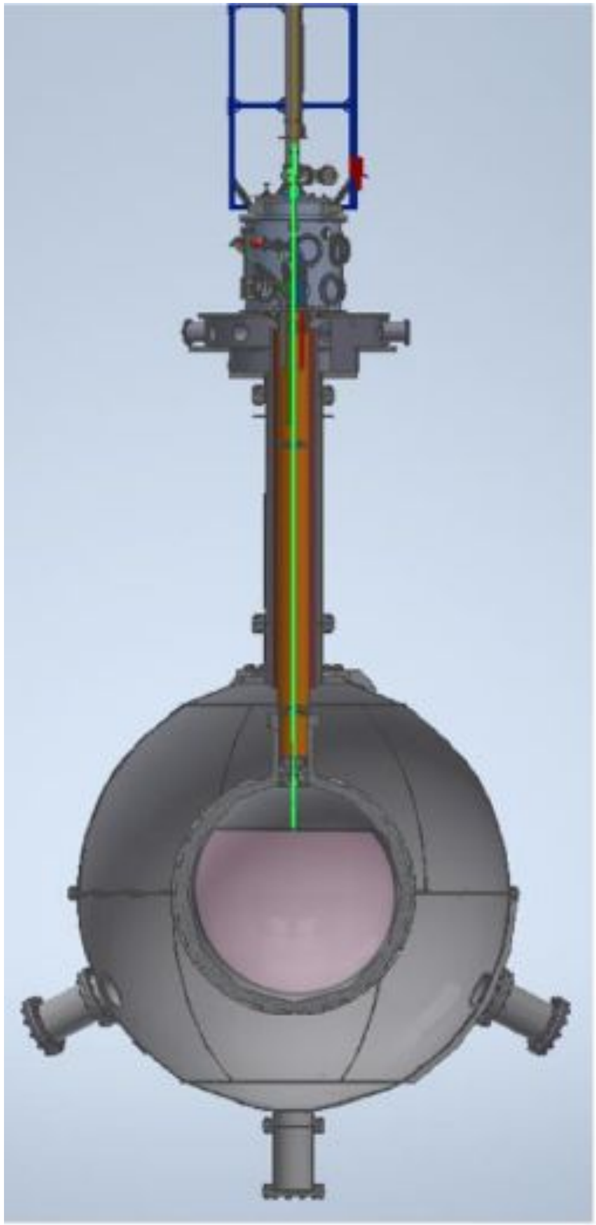

Already @ SNOLAB

# Recovering sensitivity

Upgrade to be finished early 2024

Ar fill scheduled for spring 2024

Data taking scheduled to resume in Summer 2024

Data taking for 2 more years

Finalize refined analysis and unblind

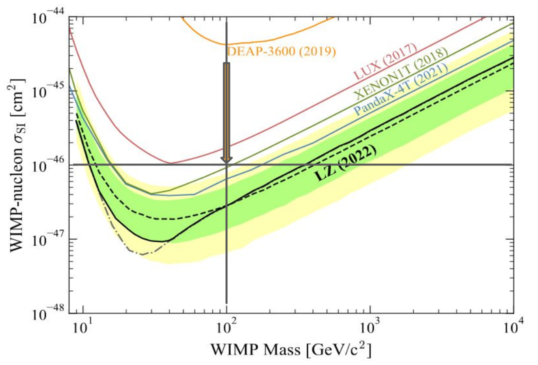

# More results

Recent precision measurement of $^{39}$Ar activity in atmospheric Ar:

$0.964 \pm 0.001_{stat} \pm 0.024_{sys}$ Bq/kg

Eur. Phys. J. C 83, 642 (2023)

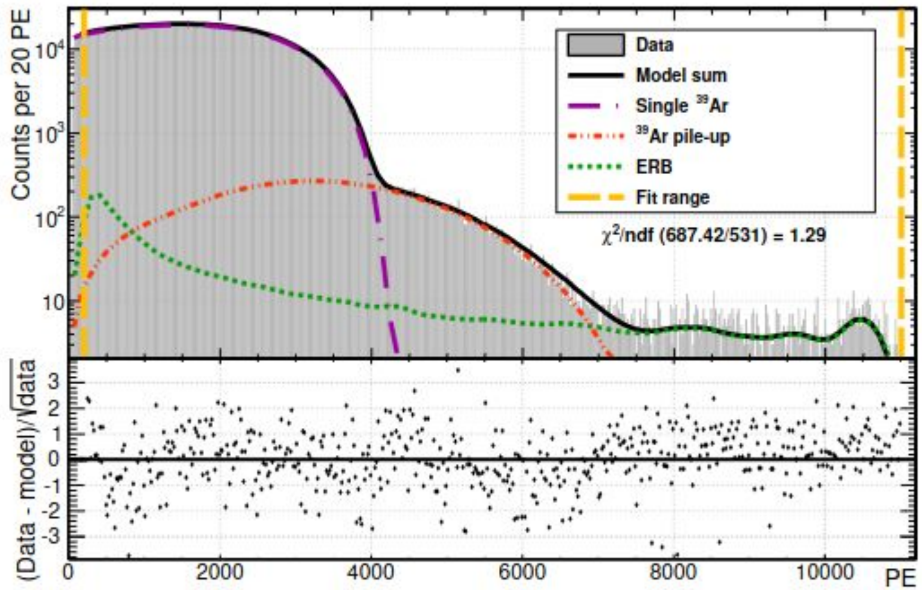


More physics in the oven:

- Solar axion search
- Solar neutrinos
- Half life of $^{39}$Ar
- Alpha scintillation quenching
- Search for Boosted DM
- Muon flux and instrumentation

DEAP 3600

ASTROCENT

UNIVERSITY OF ALBERTA

Canadian Nuclear Laboratories
Laboratoires Nucléaires Canadiens

Carleton UNIVERSITY

UC RIVERSIDE

US University of Sussex

Particle Physics
Rutherford Appleton Laboratory

GOBIERNO DE ESPAÑA
MINISTERIO DE CIENCIA, INNOVACIÓN Y UNIVERSIDADES
Ciemat
Centro de Investigaciones Energéticas, Medioambientales y Tecnológicas

LaurentianUniversity
UniversitéLaurentienne

PRINCETON UNIVERSITY

ROYAL HOLLOWAY UNIVERSITY OF LONDON

Technical University of Munich
TUM

INFN
Istituto Nazionale di Fisica Nucleare

NATIONAL RESEARCH CENTER "KURCHATOV INSTITUTE"

IF
Instituto de Física

Queen's UNIVERSITY

SNOLAB

TRIUMF

# Backup

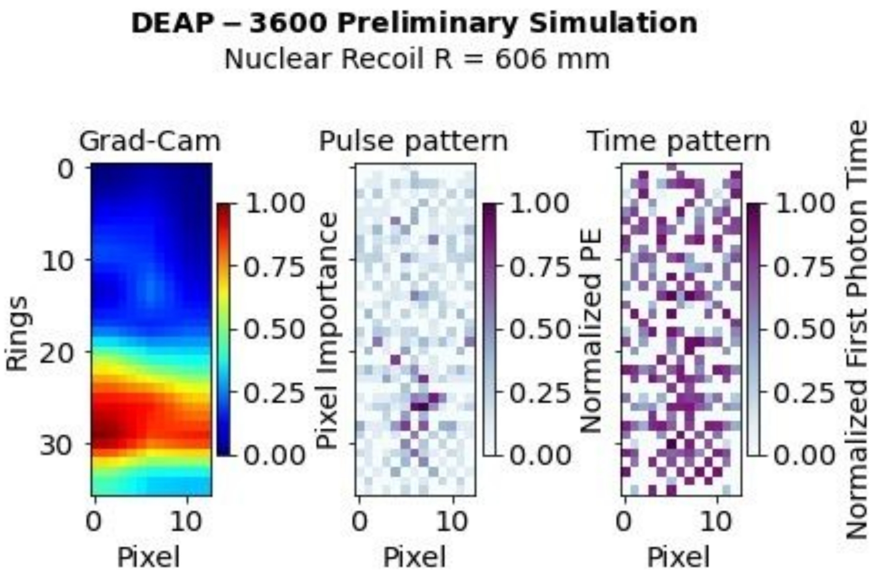
DEAP – 3600 Preliminary Simulation
Nuclear Recoil R = 606 mm
Grad-Cam
Pulse pattern
Time pattern
Rings
Pixel
Pixel Importance
Normalized PE
Normalized First Photon Time
1.00
0.75
0.50
0.25
0.00

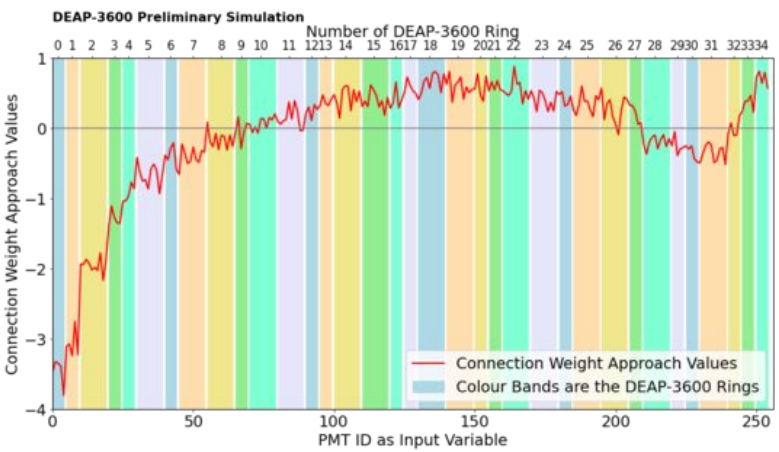
DEAP-3600 Preliminary Simulation
Number of DEAP-3600 Ring
Connection Weight Approach Values
PMT ID as Input Variable
Connection Weight Approach Values
Colour Bands are the DEAP-3600 Rings

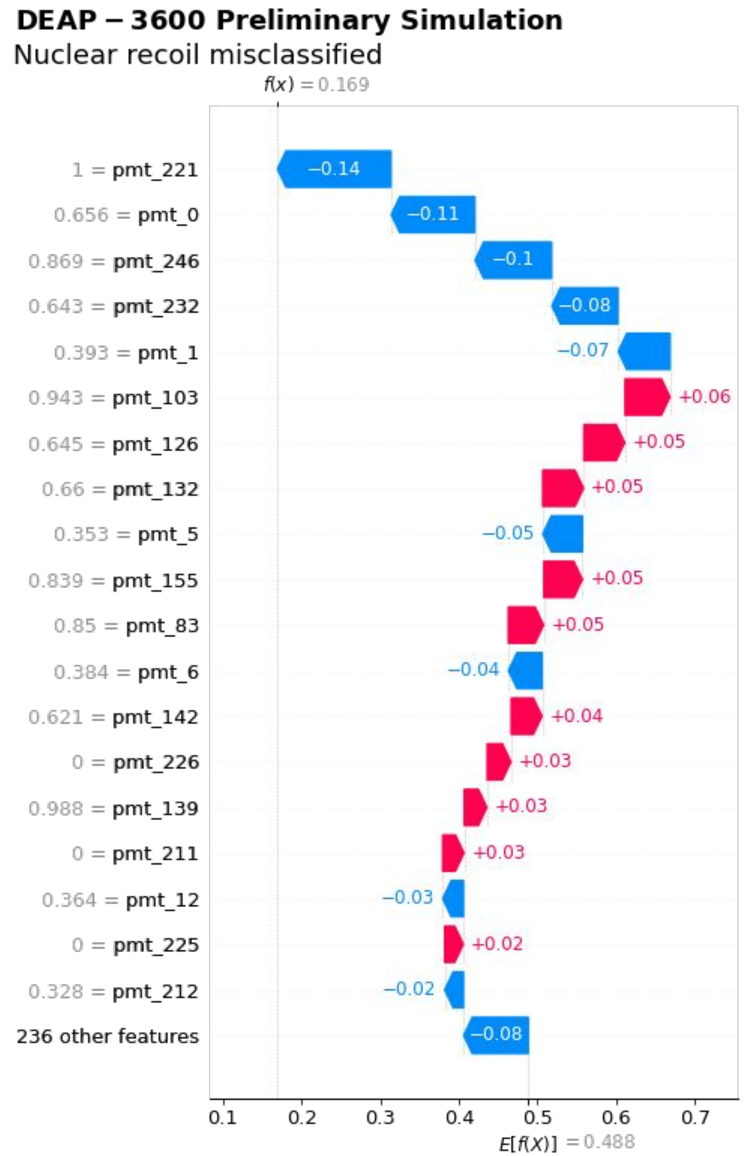
DEAP – 3600 Preliminary Simulation
Nuclear recoil misclassified
f(x) = 0.169
1 = pmt_221
0.656 = pmt_0
0.869 = pmt_246
0.643 = pmt_232
0.393 = pmt_1
0.943 = pmt_103
0.645 = pmt_126
0.66 = pmt_132
0.353 = pmt_5
0.839 = pmt_155
0.85 = pmt_83
0.384 = pmt_6
0.621 = pmt_142
0 = pmt_226
0.988 = pmt_139
0 = pmt_211
0.364 = pmt_12
0 = pmt_225
0.328 = pmt_212
236 other features
−0.14
−0.11
−0.1
−0.08
−0.07
+0.06
+0.05
+0.05
−0.05
+0.05
+0.05
−0.04
+0.04
+0.03
+0.03
+0.03
−0.03
+0.02
−0.02
−0.08
E[f(X)] = 0.488

# Current picture

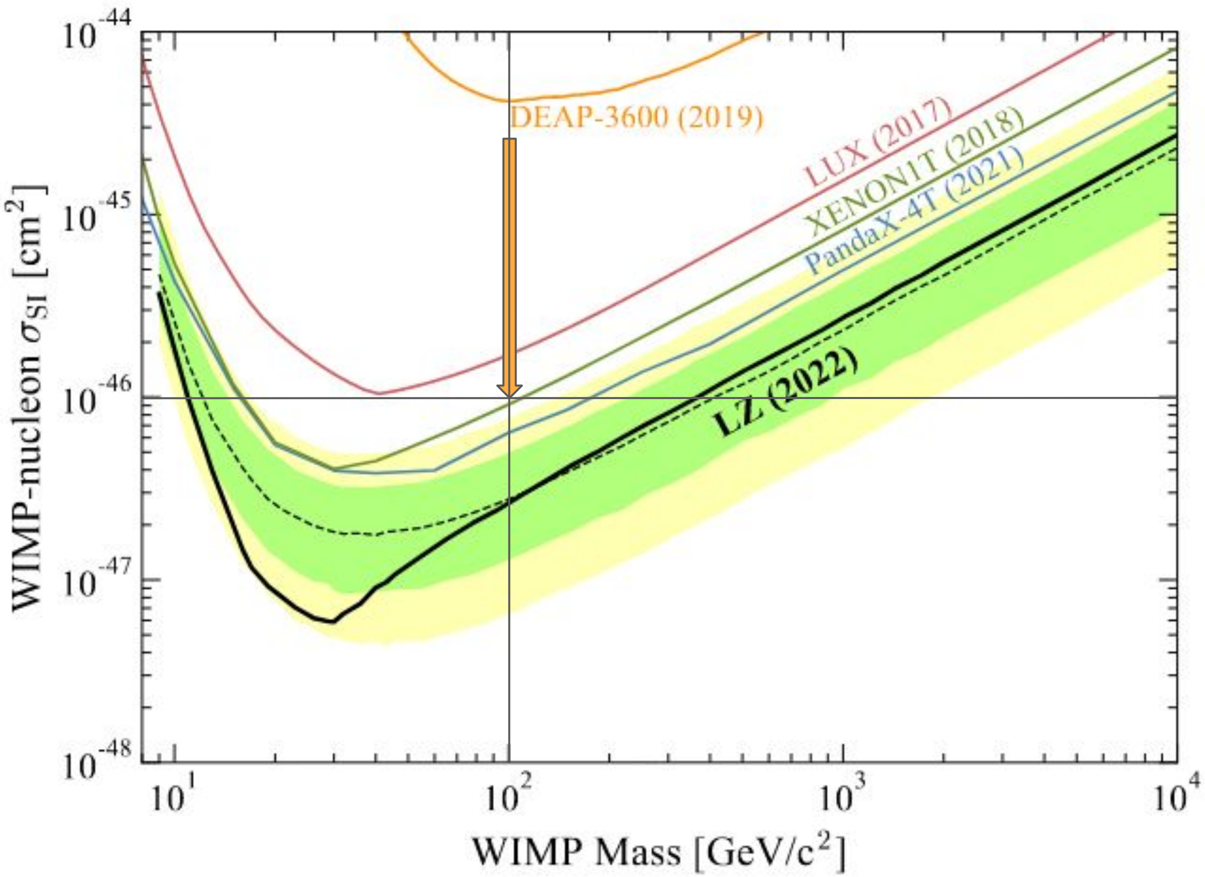


Broadly accepted picture… which relies on two unknowns:

- Standard Halo Model
- DM-nucleon coupling

which is not essentially bad, but worth keeping an eye on

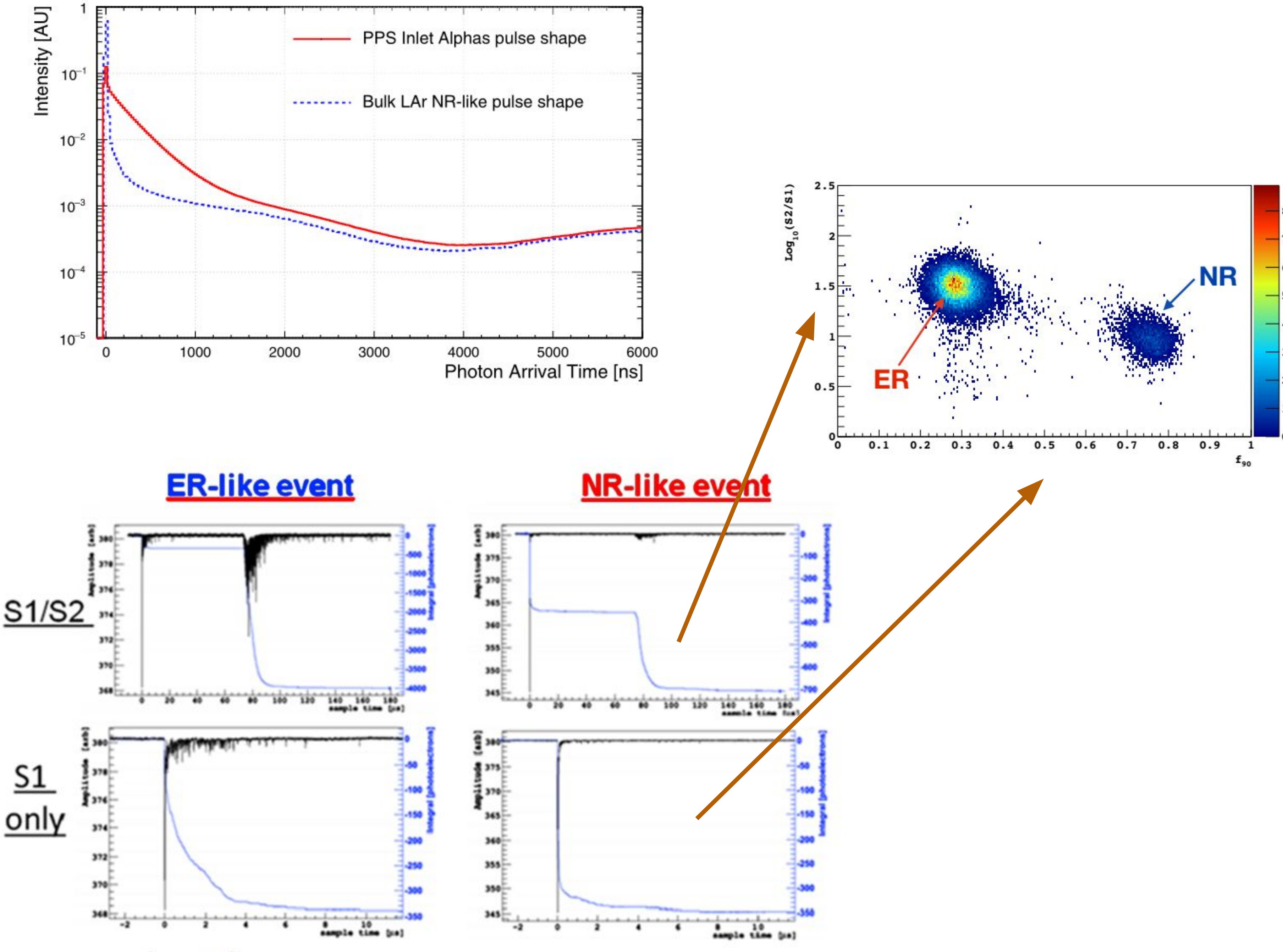
Intensity [AU]
PPS Inlet Alphas pulse shape
Bulk LAr NR-like pulse shape
Photon Arrival Time [ns]
ER
NR
f90
ER-like event
NR-like event
S1/S2
S1
only

# Exploring different scenarios

$$\frac{dR}{dE_R} = \frac{\rho_T}{m_T}\frac{\rho_\chi}{m_\chi}\varepsilon(E_R)\int_{v_{\min}}^{\infty} v f_\chi^{\oplus}(\vec{v})\frac{d\sigma}{dE_R}d^3\vec{v}$$

Recoil rate in Ar for

different WIMP distributions

| | Substructure | Type | Reference |
|---|---|---|---|
| | *Gaia* Sausage (Necib *et al.*) | Debris flow | [60] |
| | *Gaia* Sausage (O'Hare *et al.*) | Debris flow | [17] |
| G1 | Koppelman 1[a] | Stream | [19] |
| | IC ($\pi$, 400 km/s) | IC | ... |
| G2 | S1[a] | Stream | [17] |
| | Koppelman 2 | Stream | [19] |
| | IC ($\pi$, 300 km/s) | IC | ... |
| G3 | IC ($\pi$, 200 km/s)[a] | IC | ... |
| | IC ($\frac{\pi}{2}$, 400 km/s) | IC | ... |
| G4 | IC ($\frac{\pi}{2}$, 300 km/s)[a] | IC | ... |
| G5 | Helmi[a] | Stream | [19] |
| | IC ($\frac{\pi}{2}$, 200 km/s) | IC | ... |
| G6 | Nyx[a] | Stream | [18] |
| | IC (0, 400 km/s) | IC | ... |
| | IC (0, 300 km/s) | IC | ... |
| | IC (0, 200 km/s) | IC | ... |

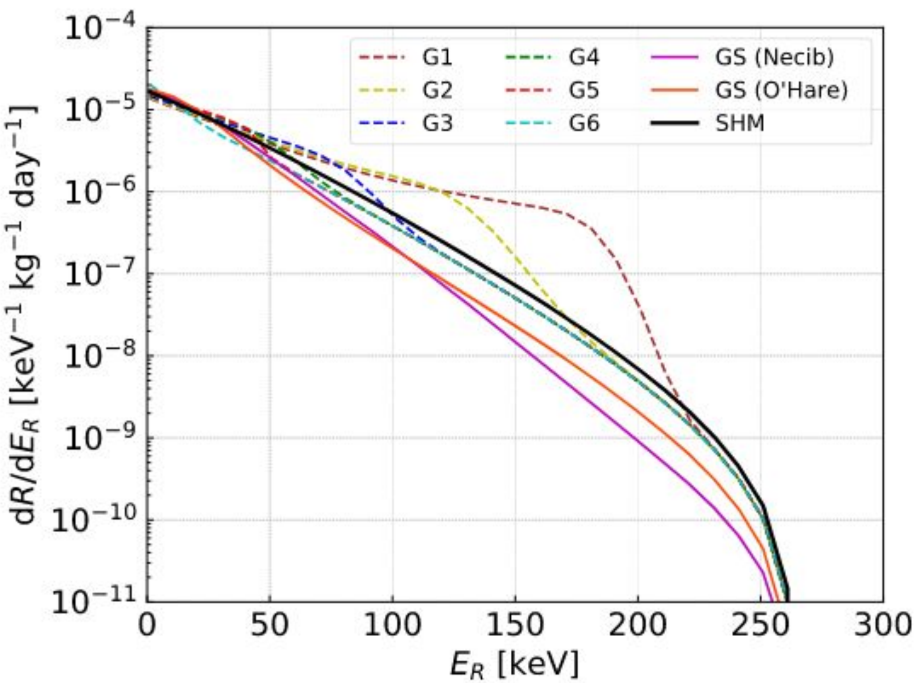


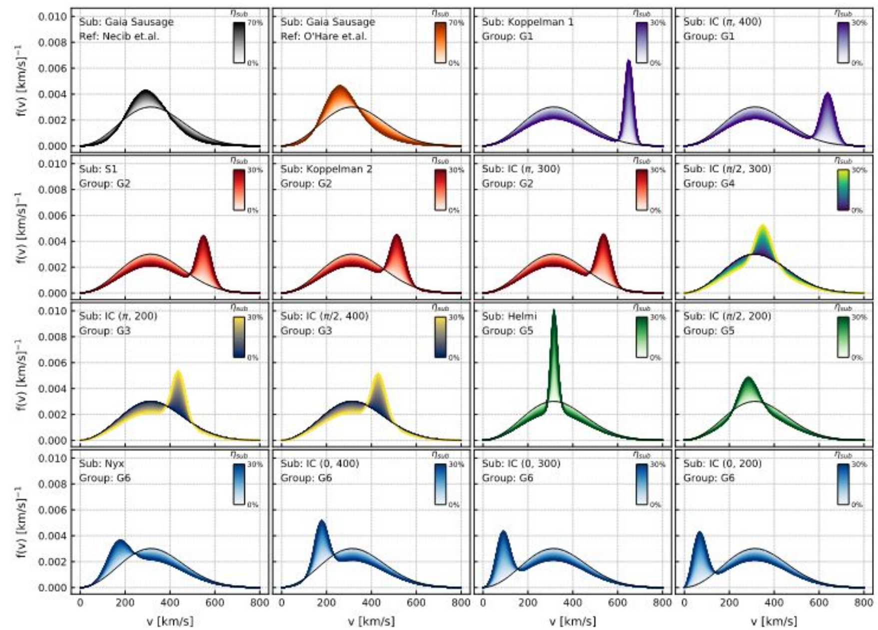


Phys. Rev. D 102, 082001 – Published 22 October 2020; Erratum Phys. Rev. D 105, 029901 (2022)'

# Exploring different scenarios

Recoil rate in Ar for

$$\mathcal{L}_{\text{int}} = \sum_{N=n,p} \sum_i c_i^{(N)} \mathcal{O}_i \chi^+ \chi^- N^+ N^-$$

different non-relativistic effective operators

Phys. Rev. D 102, 082001 – Published 22 October 2020; Erratum Phys. Rev. D 105, 029901 (2022)'

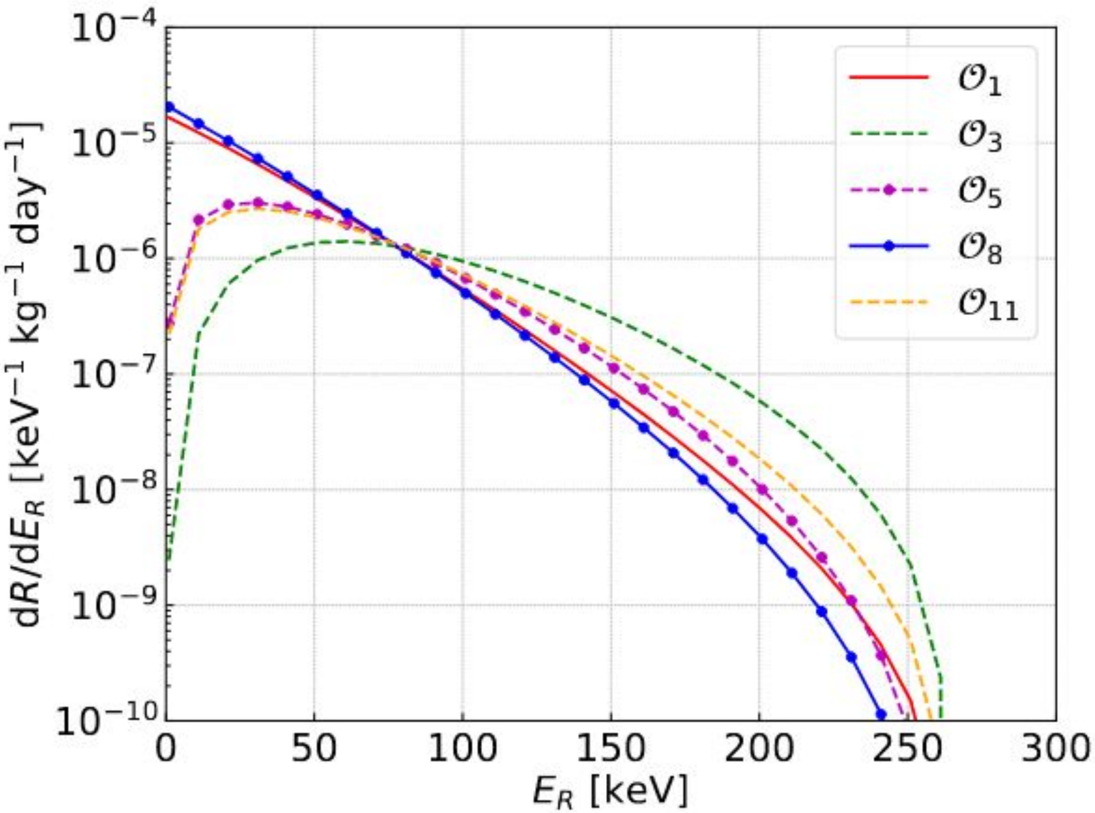


$$\mathcal{O}_1 = 1_\chi 1_N,$$

$$\mathcal{O}_3 = i\vec{S}_N \cdot \left(\frac{\vec{q}}{m_N} \times \vec{v}_\perp\right),$$

$$\mathcal{O}_5 = i\vec{S}_\chi \cdot \left(\frac{\vec{q}}{m_N} \times \vec{v}_\perp\right),$$

$$\mathcal{O}_8 = \vec{S}_\chi \cdot \vec{v}_\perp,$$

$$\mathcal{O}_{11} = i\vec{S}_\chi \cdot \frac{\vec{q}}{m_N},$$

# Exploring different scenarios

- Mχ = 100 GeV/c^2.
- Isoscalar coupling (cp = cn).
- Arbitrary cross section considered, just for comparison of shapes.

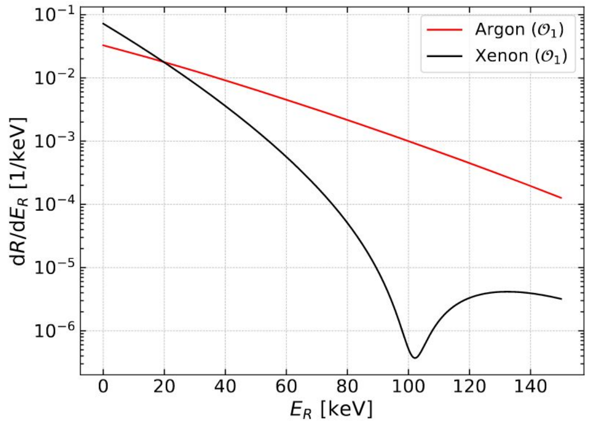


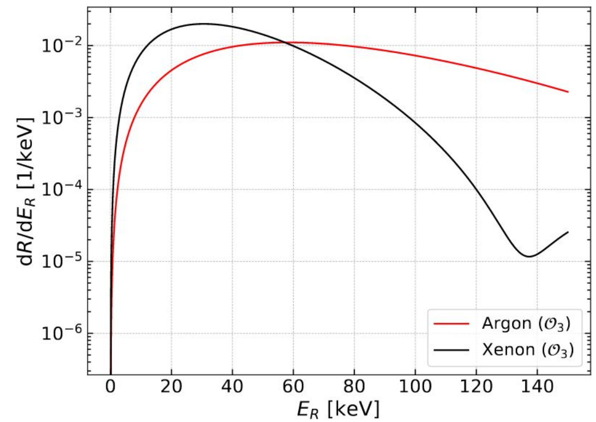


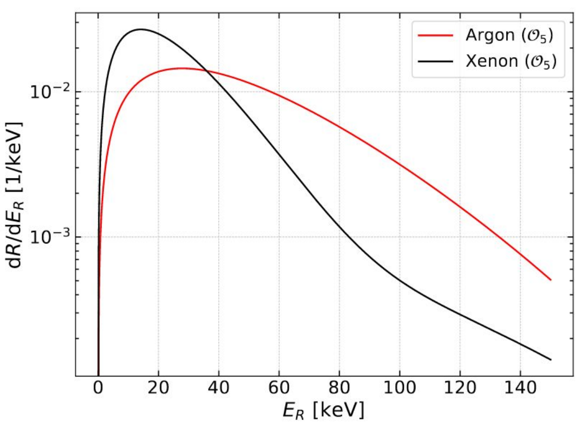


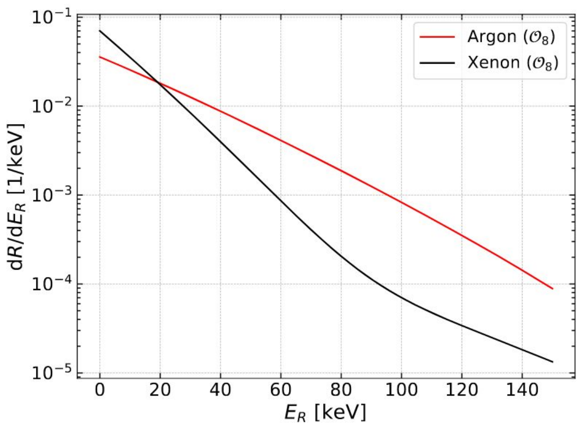


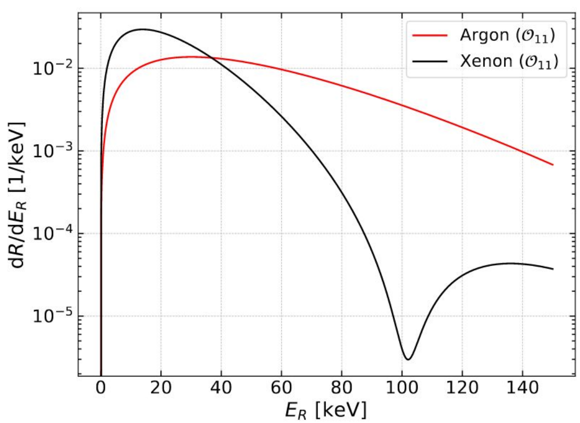

# Exploring different scenarios

**Recoil rate in Ar for**

different $c_i^0$ / $c_i^1$ escenarios

Phys. Rev. D 102, 082001 – Published 22 October 2020; Erratum Phys. Rev. D 105, 029901 (2022)’

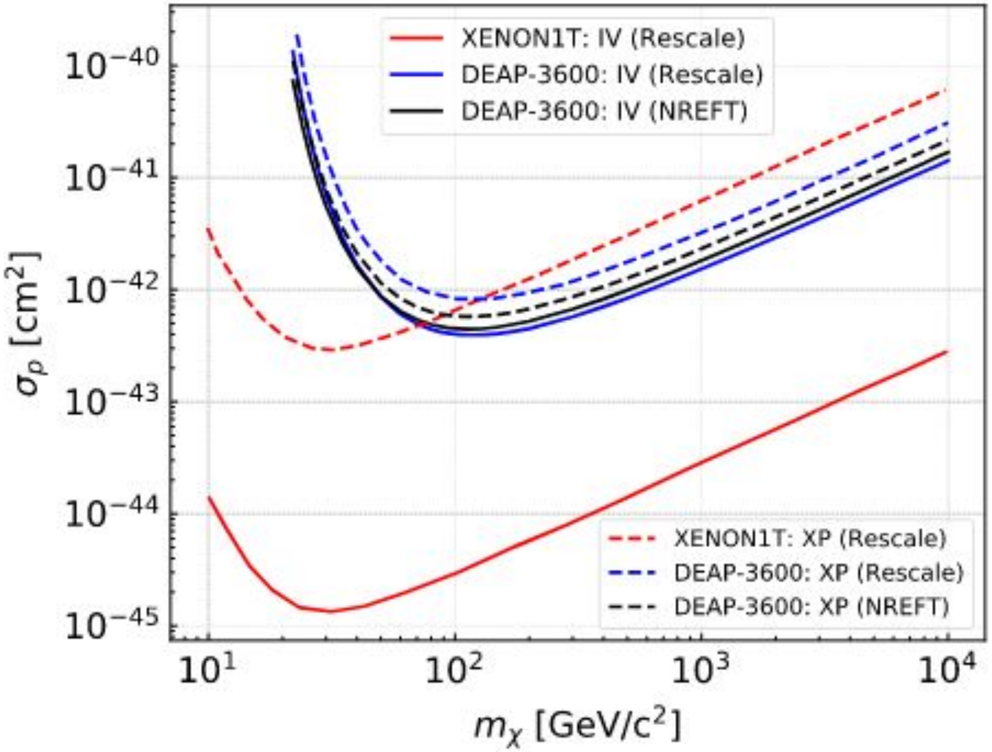


$$c_i^p \equiv (c_i^0 + c_i^1)/2$$

$$c_i^n \equiv (c_i^0 - c_i^1)/2$$

IS $\quad c_i^n = c_i^p$

IV $\quad c_i^n = -c_i^p$

XP $\quad c_i^n / c_i^p = -0.7$

# Exploring different scenarios


[17] C. A. J. O'Hare, N. W. Evans, C. McCabe, G. C. Myeong, and V. Belokurov, Velocity substructure from *Gaia* and direct searches for dark matter, Phys. Rev. D **101**, 023006 (2020).

[18] L. Necib *et al.*, Evidence for a vast prograde stellar stream in the solar vicinity, arXiv:1907.07190.

[19] L. Necib *et al.*, Chasing accreted structures within Gaia DR2 using deep learning, arXiv:1907.07681.

[60] L. Necib, M. Lisanti, and V. Belokurov, Inferred evidence for Dark Matter Kinematic Substructure with SDSS–*Gaia*, Astrophys. J. **874**, 3 (2019).


| | Substructure | Type | Reference | $v_r$ (km/s) | $v_\theta$ | $v_\phi$ | $\lvert\sigma_{rr}\rvert$ (km/s) | $\lvert\sigma_{\theta\theta}\rvert$ | $\lvert\sigma_{\phi\phi}\rvert$ | $\eta_{\rm sub}$ |
|---|---|---|---|---|---|---|---|---|---|---|
| | *Gaia* Sausage (Necib *et al.*) | Debris flow | [60] | $\pm 147^{+7.2}_{-6.4}$ | $-2.8^{+1.5}_{-1.6}$ | $27.9^{+2.8}_{-2.9}$ | $113.6^{+3.1}_{-3.0}$ | $65.2^{+1.1}_{-1.2}$ | $61.9^{+2.6}_{-2.9}$ | 0–0.70 |
| | *Gaia* Sausage (O'Hare *et al.*) | Debris flow | [17] | −8.2 | 0.99 | 25.7 | 158.9 | 80.9 | 61.5 | 0–0.70 |
| G1 | Koppelman 1[a] | Stream | [19] | −169 | −59 | −375 | 11–37 | 3–16 | 6–28 | 0–0.30 |
| | IC ($\pi$, 400 km/s) | IC | ··· | 0 | 0 | −400 | 35.4 | 35.4 | 30 | 0–0.30 |
| G2 | S1[a] | Stream | [17] | −29.6 | −72.8 | −297.4 | 82.6 | 58.5 | 26.9 | 0–0.30 |
| | Koppelman 2 | Stream | [19] | 213 | 161 | −226 | 52 | 18 | 29 | 0–0.30 |
| | IC ($\pi$, 300 km/s) | IC | ··· | 0 | 0 | −300 | 35.4 | 35.4 | 30 | 0–0.30 |
| G3 | IC ($\pi$, 200 km/s)[a] | IC | ··· | 0 | 0 | 200 | 35.4 | 35.4 | 30 | 0–0.30 |
| | IC ($\frac{\pi}{2}$, 400 km/s) | IC | ··· | 282.8 | 282.8 | 0 | 21.2 | 21.2 | 50 | 0–0.30 |
| G4 | IC ($\frac{\pi}{2}$, 300 km/s)[a] | IC | ··· | 212.1 | 212.1 | 0 | 21.2 | 21.2 | 50 | 0–0.30 |
| G5 | Helmi[a] | Stream | [19] | 29 | −287 | 141 | 37–83 | 6–21 | 4–15 | 0–0.30 |
| | IC ($\frac{\pi}{2}$, 200 km/s) | IC | ··· | 141.4 | 141.4 | 0 | 21.2 | 21.2 | 50 | |
| G6 | Nyx[a] | Stream | [18] | $156.8^{+2.1}_{-2.2}$ | $-1.4^{+3.1}_{-3.0}$ | $141.0^{+2.5}_{-2.6}$ | $46.9^{+1.7}_{-1.6}$ | $70.9^{+2.4}_{-2.2}$ | $52.5^{+1.8}_{-1.8}$ | 0–0.30 |
| | IC (0, 400 km/s) | IC | ··· | 0 | 0 | −400 | 35.4 | 35.4 | 30 | 0–0.30 |
| | IC (0, 300 km/s) | IC | ··· | 0 | 0 | −300 | 35.4 | 35.4 | 30 | 0–0.30 |
| | IC (0, 200 km/s) | IC | ··· | 0 | 0 | −200 | 35.4 | 35.4 | 30 | 0–0.30 |

# Axion interactions in DEAP-3600 produce EM events

- **Compton conversion**
  - Get 1 gamma and 1 electron, with 5.5 MeV total kinetic energy
- **Inverse Primakov**
  - Get 1 gamma with 5.5 MeV energy
- **Axio-electric effect**
  - Get 1 electron with 5.5 MeV kinetic energy
- **Axion decay into 2 gammas**
  - Get 2 gammas with 5.5 MeV total energy

Compton Conversion

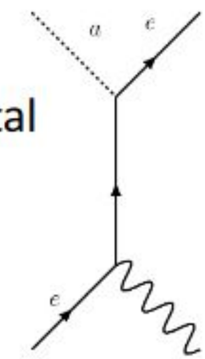


Decay to $2\gamma$

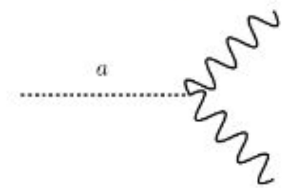


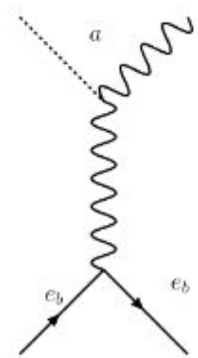


Inverse Primakov

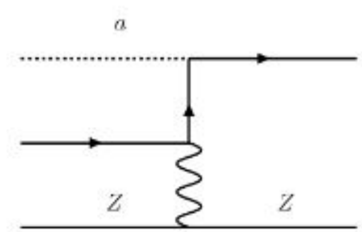


Axio-Electric Effect